Tailored coating of gold nanostars: a rational approach to a prototype of theranostic device based on SERS and photothermal effects at ultralow irradiance.

B.Bassi,[1]G. Dacarro,[1] P. Galinetto, [2] E. Giulotto,[2] N. Marchesi,[3] P. Pallavicini,[1] A. Pascale,[3] S. Perversi[1] and A. Taglietti[1*]

1) Dipartimento di Chimica, Sezione di Chimica Generale, Università di Pavia, viale Taramelli, 12 - 27100 Pavia – Italy;
2) Dipartimento di Fisica "A.Volta", Università di Pavia, Via Bassi 6, - 27100 Pavia – Italy;
3) Dipartimento di Scienze del Farmaco, Sezione di Farmacologia, Università di Pavia, viale Taramelli, 14 - 27100 Pavia – Italy.
Corresponding Author: * E-mail: angelo.taglietti@unipv.it.

Abstract. The last decade came across an increasing demand of theranostic biocompatible nanodevices, possessing the double ability of diagnosis and therapy. In this work, we report the design, synthesis and step-by-step characterization of rationally coated gold nanostars (GNS) for SERS imaging and photothermal therapy (PTT) of HeLa cancer cells. The nanodevice was realized synthesizing GNS with a seed-growth approach, coating them with a controlled mixture of thiols composed of a Raman reporter and a polyethylenglicol with a terminal amino group, and then reacting these amino groups with Folic Acid (FA), in order to impart selectivity towards cancer cells which overexpress folate receptors on their membranes. After a complete characterization, we demonstrated that these FA functionalized GNS (FA-GNS) are able to bind selectively to membranes of HeLa cells, acting as SERS tags and allowing SERS imaging. Moreover, we demonstrated that once bound to HeLa cells membranes, FA-GNS show a photothermal effect which can be exploited to kill the same cells *in vitro* using a laser irradiation in the NIR at a very low and safe irradiance. We thus demonstrated that FA-GNS designed following the described approach are an efficient prototype of theranostic nanodevice.

.

Keywords SERS, Gold Nanostars, surface modification, mixed monolayers, photothermal therapy, theranostics

1. Introduction

Gold nanoparticles (GNP) show enormous potential in biomedical applications, nanomedicine and development of theranostic devices.[1,2] One of the most intriguing features of GNP is the tunability of their shapes and dimensions, which determines their plasmonic features. Indeed, the Localized Surface Plasmon Resonance (LSPR) absorption band of gold anisotropic nanoparticles like gold nanorods (GNR) and gold nanostars (GNS) can be finely tuned in the desired spectral window regulating the synthetic parameters.[3,4] Surface Enhanced Raman Scattering (SERS) takes advantage from plasmonic features and allows to dramatically enhance the Raman signal of molecules when placed in close proximity to a nanosized noble metal structure. Thus, SERS is used in a very wide range of applications, for example in the biomedical imaging, with “SERS tags” which had become an alternative to fluorescence tagging.[5] SERS tags are based on noble metal nanoparticles able to recognize a specific target (for example a cell), signaling the recognition with the intense SERS spectra of a properly chosen molecule grafted on the surface of the device itself.

The photothermal effect is at the basis of photothermal therapy (PTT). [6] Using PPT target cancer or bacterial cells can be destroyed by laser irradiation of plasmonic nanoobjects located in the close surroundings of the target. Different kind of nanodevices have been proposed as PTT agents: gold nanostructures, [7,8] other inorganic nanoparticles [9,10] and carbon based nanoparticles.[11] Among these nanoplatforms, GNS are particularly indicated as their plasmon properties can be finely tuned by changing the length and the architecture of branches, and thus can be easily placed where desired in the NIR region, in the so called biological window, in which tissues are transparent.[3,4] Moreover, branches and tips offered by GNS provoke the so-called “lightning rod” effect. The SERS signals of molecules close to anisotropic GNP are further enhanced with respect than those from spherical or symmetric GNP just due the very high electric yield intensities experienced in that zones.[2, 12] It results thus evident that GNS and more generally anisotropic branched gold nano-objects can be exploited as efficient cores both for SERS-based imaging and PPT: they are perfect as starting materials for the realization of prototypes of theranostic devices, and some examples of SERS tags for imaging and photothermal destruction of cancer cells based on these nano-objects appeared in the last years, [12-16] in some cases demonstrating their superior photothermal conversion efficiency

when compared to GNR.[14] Nevertheless, the development of rationally designed, reproducible, controllable and efficient new devices of this type is still strongly needed by the biomedical community.

The components of a robust and efficient SERS tag must be carefully chosen. Firstly, a noble metal nanoparticle must guarantee a strong enhancement factor (EF) for the Raman signal. As already introduced, GNS have showed optimal EF's, due to the presence of branches and tips that ensure SERS hot spots. The second component needed is a Raman reporter, a molecule with an intrinsic high Raman cross-section, which should be strictly bound to the metal surface of the nanoparticle, in order to prevent its detachment in presence of chemical species competing for the surface affinity: usually a thiol function fits well to this task. The third component is a biocompatible layer protecting the metal nanoparticle and the Raman reporter: once more, this unit should be firmly grafted on the metal surface, and, again, a thiol function is the first choice option. The last component required is a targeting fragment, able to specifically bind to the cellular target that we want to reveal.[5]

Thus in the preparation of a SERS tag, the surface of the nanoparticle becomes the place of a competition between different actors: surface ligands originally used for the GNP synthesis and stabilization, Raman reporter molecules, biocompatible protecting units, targeting moieties. This situation must be carefully studied, to obtain a robust and reproducible nano-device: the surface "real estate" should be precisely tailored, in order to avoid drawbacks. Competitive absorption involving protecting units and Raman reporter molecules could lead to two opposite problems: uncomplete protection from biofouling (in presence of an excess of Raman reporter) or weak SERS signal (in presence of an excess of protecting units). Moreover, anisotropic nano-objects synthesis usually require the use of surfactants, which can be toxic: an incomplete surface functionalization will result in the incomplete elimination of harmful chemicals, and this is another obvious problem when thinking to biological applications. Thus, one should know and control exactly the concentrations of molecules needed to give full coverage to the monolayers and the compositions of the mixture of Raman reporter, and protect units brought on surface of SERS tags. As we[17,18] and others[19] have recently demonstrated, the coating of noble metal nano-objects with mixed monolayers of thiols can be sharply controlled in a simple way. Therefore, robust SERS probes can be prepared modulating the quantity of different protecting units and of Raman reporter brought on surface, thus controlling precisely the SERS signal intensity and maintaining an overall stability in biological conditions.[17]

In the present paper, we will describe the realization of a prototype of theranostic device based on the considerations introduced so far, and exploiting folic acid (FA) as targeting group. FA, a

vitamin involved in several cellular metabolic pathways and essential for nucleotide biosynthesis, represents a good alternative to protein or antibodies based targeting moieties, as it is more stable and less prone to aggregation with components of human serum.[20] Moreover, the design of a folate-targeted delivery system can allow reaching a high drug concentration at the site of tumour cells with low systemic exposure.[21] Folate receptors (FRs), which are able to internalize FA, are overexpressed in several types of human cancer cells like HeLa,[22] OV-167[23] and GP-38,[24] to name a few. FA has other advantages: it is low-cost, it has non-immunogenic properties, and it is ready to be easily conjugated to other molecules, for example exploiting its carboxylic groups. In a smart, recent example, Silver nanoplates coated with chitosan, conjugated with FA and SERS-labelled with a proper Raman reporter were used for multimodal detection and targeted PTT of cancer cells.[25] We choose a thiolated poly-oxoethylene glycol (PEG), HS-PEG_{3000}-NH_2, as it possess a thiol function for grafting on gold surface and a terminal primary amine ready for reaction with the carboxylic functions of FA molecules by means of simple and quantitative coupling reactions. As a Raman reporter, we choose 7-mercapto-4-methylcoumarin (MMC), as its high Raman cross-section and peculiar Raman fingerprint are coupled with the presence of a thiol moiety, fitting the already explained features for an efficient SERS reporter molecule.[17,18]

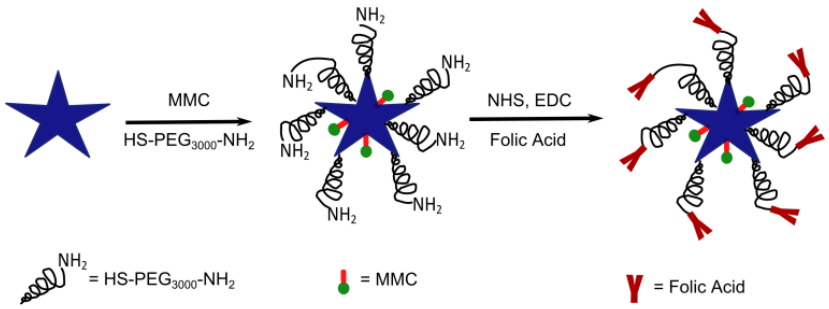

Scheme 1 Synthetic strategy used for the preparation of FA-GNS

We will show the synthesis and the step-by-step characterization of the device, its ability to discriminate HeLa cancer cells overexpressing FR from normal healthy cells, its ability to act as a SERS tag for imaging of cancer cells, and the efficiency of *in vitro* PTT, demonstrating that this theranostic device is able to kill cancer cells by localized hyperthermia at an ultralow (< 0.2 W/cm^2) power laser density, below the limit (0.4 W/cm^2) which is considered as the maximal permissible exposure of skin.[26]

2. Methods

2.1 Chemicals

N-Dodecyl-N,N-dimethyl-3-ammoniun-1-propansulfunate (LSB) (≥99.7%), Gold(III) chloride trihydrate (~30wt% in HCl 99.99%), sodium borohydride (98%), L-ascorbic acid (≥99%), silver nitrate (99.8%), 7-mercapto-4-methylcoumarin (MMC) ≥97%, ethanol (≥99.8 %), sodium hydroxide (≥98%), nitric acid (1N), chloridric acid (37%) folic acid (FA) (≥97%), triethylamine (≥99%), N-(3-dimethylaminopropyl)-N-ethylcarbodiimide (EDC) (≥99%), N-hydroxysuccinimide (NHS) (98%), dimethylsulfoxide anhydrous (DMSO) (≥99%), N,N′-dicyclohexylcarbodiimide (DCC) 99% were all purchased from Sigma-Aldrich. SH-PEG_{3k}-COOH (poly(ethylene glycol) 2-mercaptoethyl ether acetic acid) and SH-PEG_{3k}-NH_2 (α-mercapto-ω-amino poly(ethyleneglycol) hydrochloride) were purchased from RAPP polymers. Reagents were used as received. All the preparations were made with bi-distilled water.

2.2 Instruments

UV-Vis spectra were taken on Cary 60 Varian, using quartz or poly(methyl methacrylate) cuvettes (optical path 1 cm). The wavelength scan range was 300-1100 nm. Ultracentrifugation was performed with the ultracentrifuge HermleZ366 using polypropylene 10mL tubes. Dynamic light scattering (DLS) size and Z-potential characterization were operated with a Zetasizer Nano-ZS90 (source: polarized He–Ne laser, 30 mW output power, vertically polarized). The concentration of gold was detected using ICP-OES (inductively coupled plasma optical emission spectroscopy) with a OPTIMA 3000 Perkin Elmer instrument. Transmission electron microscopy (TEM) characterization was performed using Jeol LEM-1200 EX II instrument. Samples were obtained from diluted 10 μL colloidal solution drops deposited on Copper grids (300 mesh) covered with Parlodion membrane. SERS spectra were obtained at room temperature with a Labram Dilor H10 spectrometer equipped with an Olympus microscope HS BX40. FT-IR spectrum 100 Perkin Elmer was used to acquire infrared spectra. A multimode AlGaAs laser diode, L808P200 from Thorlabs GmbH, with an emission wavelength of about 808 nm, 150 mW of power radiation, was used for irradiation.

2.3 Synthesis of GNS

GNS were synthesized using a previously reported method.[4] Briefly, a colloidal suspension of seeds was prepared by adding equal amounts of an aqueous solution of $HAuCl_4$ ($5.0x10^{-4}$ M) and of an aqueous solution of LSB (0.20 M) in vial. After that, an ice-cooled solution of $NaBH_4$ in water (0.01 M, 600 μL) was added to 10 mL of the pale yellow solution of $AuCl_4^-$ obtained in the previous step. The resulting solution (brown-orange) was hand-shaken carefully for a few seconds. In the same time, a growth solution was prepared gently mixing 50 mL of 0.20 M LSB

solution in water, $AgNO_3$ in water (0.0040 M, 1800 µL), aqueous $HAuCl_4$ (0.0010 M, 50 mL) and aqueous L-ascorbic acid solution (0.0780 M, 820 µL) obtaining, after a short time, a colourless solution. To this solution, the proper quantity of seeds suspension (120 µL) was added. The reaction mixture was allowed to react for 1 h without stirring: development of a typical dark blue colour was observed. The obtained suspensions can be stored at room temperature in the preparation vessel, kept in the dark and used within 7 days. To be used for functionalizations, successive coatings and reactions, the samples had to be ultra-centrifuged (13000 rpm, 25 min), with successive discarding of the supernatant: at this point the precipitated pellet could be re-suspended in the same starting volume of bi-distilled water and used for further steps.

2.4 Spectrophotometric titrations of GNS with HS-PEG_{3k}-NH_2

In a typical experiment, a volume 10 mL of as-prepared GNS colloid was titrated with a 10^{-3} M stock solution of HS-PEG_{3k}-NH_2 in water. After each addition of the titrant, the solution was mixed gently for 3 minutes before recording UV-Vis spectrum.

2.5 Coating of GNS with mixed monolayers of thiols

To a proper volume of GNS colloid (10-100 mL), a proper amount of stock solution (prepared in water in the case of PEGs or in ethanol in the case of MMC) of desired thiols was added, in order to obtain the chosen composition of the mixture and reaching the overall thiol concentration of $1.1x10^{-5}$ M. For example, the mixture containing 25% of MMC and 75% of HS-PEG_{3k}–NH_2 was obtained with the following final concentrations in the colloidal suspension: 2.75×10^{-6} M in MMC and 8.25×10^{-6} M in HS-PEG_{3000}–NH_2. Alternative coatings of GNS were achieved in similar way, 100% of HS-PEG_{3000}–NH_2 (in water) or 100% of HS-PEG_{3000}–COOH (in water) were obtained using, as final concentration in the colloidal suspension, the value of 1.1×10^{-5} M. After coating, the obtained colloidal suspension of GNS was stirred at room temperature for one night before an ultra-centrifugation (13000 rpm, 25'). After this strep and the discarding of the supernatant, re-dissolution of the obtained pellet was performed in the desired volume of bi-distilled water. This centrifugation/re-dissolutions cycle was repeated 3 times. After the last cycle the pellets were re-dissolved in the desired amount of bi-distilled water, which was calculated in order to obtain the desired concentration.

2.6 Synthesis of FA-GNS

A solution of FA 10^{-3} M in DMSO (3.0 mL) was prepared, and to this subsequently 600 µL of EDC solution 0.1 M (in DMSO) and 600 µL of NHS solution 0.1 M (in DMSO) were added. The mixture was allowed to react for 1 h at room temperature. After this step, 9 mL of coated GNS (concentrated 10x) were added. The acidity of the solution was adjusted to pH=8 with triethylamine. The mixture was allowed to react for one night under gentle stirring and then ultra-

centrifuged (13000 rpm, 25'). The supernatant was discarded and the obtained pellet re-dissolved in the same starting volume of bi-distilled water adjusted to pH=8. Ultracentrifugation/re-dissolutions cycle was repeated twice. After the last ultracentrifugation, the precipitate was re-dissolved in the amount of bi-distilled water calculated in order to obtain the desired concentration.

2.7 Cell Culture

HeLa and DI TCN1 cells were cultured in Dulbecco's modified essential medium (DMEM AQMedia, Sigma) supplemented with 10% fetal bovine serum and 1% penicillin-streptomycin at 37 °C, in an atmosphere of 5% CO_2 and 95% humidity.[27]

2.8 MTT assay

The MTT [3-(4,5-dimethylthiazol-2-yl)-2,5- diphenyltetrazolium bromide] assay (Sigma-Aldrich, Milan, Italy) was employed to evaluate mitochondrial enzymatic activity. The day before the experiment, a cell suspension of 10000 cells/well in 100 µL culture medium (DMEM+ 10%FBS+ 1x penicillin-streptomycin) was seeded into 96-well plates. After each treatment with GNS (24 hours), the medium was replaced with 100 µL of fresh medium and then, in each well, 10 µL of MTT (final concentration corresponding to 1 mg/ml) were added . Following 4 hours of incubation at 37°C, the generated purple formazan crystals were dissolved overnight at 37°C in 100 µL of Lysis Buffer [sodium dodecyl sulphate (20%) in dimethylformamide/water 1:1]. Absorbance values at 595 nm were assessed by a microplate reader (SynergyHT, BioTek Instruments, Inc.), and the data were expressed as % of the control value (100%). The analysis of variance (ANOVA) was performed on the obtained results and it was followed, when significant, by an appropriate *post-hoc* comparison test, as reported in the figure legends. When p values were ≤ 0.05, the differences were considered statistically significant.

2.9 SERS measurements

SERS spectra were acquired using the He-Ne 632.8 nm laser line as the excitation radiation. An Olympus microscope HS BX40 allowed micro-sampling. The spectrometer was equipped with a 1800 g/mm grating and a cooled CCD camera was used as photo-detector. The overall spectral resolution was about 1 cm^{-1}. A 10x objective with a 2.8 mm spot diameter was used for colloidal samples (with Au concentrations of about $2.0 \acute{} 10^{-4}$ M, corresponding to 1.3×10^{-9} M of GNS) while spectra from cells were measured by means of 50x objective with a 1.5 mm laser spot diameter. The focus depth was about 150 mm and 15 mm for 10x and 50x respectively. Different power densities were used for for colloidal samples and cells: about 5×10^5 W/cm^2 and 8×10^4 W/cm^2, respectively. Typical integration times were about 20 s and the run was repeated 5 times. The

estimation of the SERS enhancement factor was performed by comparing the SERS signal of MMC from colloidal samples with Raman signal of MMC diluted at 10^{-2} M in ethanol. The integrated intensities of the Raman modes considered for EF estimation were derived by the best-fitting procedure using lorentzian curves as fitting functions. We underline that no Raman signals from cells were measured at the experimental conditions used for SERS measurements from MMC.

2.10 Incubation of cells with FA-GNS SERS tags for SERS measurements

100000 cells were seeded on a rounded glass (Ø 2 cm) positioned over a petri dish (Ø 35 mm), 2 mL of medium (DMEM+ 10%FBS+ 1x Pen Strep) were added and left overnight at 37°C. The next day the medium was substituted with 2 mL of the colloidal samples (50 µg/mL of GNS in medium) and left 24 hours at 37°C, and after this time the sample was washed two times with PBS. Subsequently, the cells were immobilized with ethanol (70%) for 20 minutes and with formaldehyde (4%) for other 20 minutes. Then the cells were washed with PBS for two times and then the petri was filled with 2 mL of bi-distilled water.

2.11 Evaluation of photo-thermal effects

30000 cells were seeded on a rounded glass (Ø 1 cm) blocked with poly-L-lysine over a petri dish (Ø 35 mm), 2 mL of medium (DMEM+ 10%FBS+ 1x Pen Strep) were added and left overnight at 37°C. The next day the medium was substituted with 2 mL of the colloid (25 or 50 µg/mL of GNS in medium) samples and left 24 hours at 37°C, after this time each sample was washed two times with PBS and finally the petri was filled with 2 mL of PBS. Then the rounded glass were irradiated with laser (150 mW, irradiance 190 mW/cm^2 – 10 minutes) and photographed through a traditional optical microscope.

3 Results and discussion

3.1 Synthesis and characterization of SERS tag

GNS were synthesized using our previously reported method, following a seed-growth approach based on the LSB surfactant as the directing and protecting agent.[4] The absorption spectrum of GNS derives from the overlapping of three distinct plasmonic bands, the short (520-530 nm), the intermediate (620-670 nm) and the long (750-1100 nm) band, which respectively correspond to (i) nanospheres (20 nm diameter, minor component); (ii) nanostars with four trapezoidal branches (minor component); (iii) branched asymmetric NPs (prevalent component), which have narrow, long branches of high aspect ratio (AR). The position of the maximum absorption of the long band can be regulated changing the synthetic parameters,[3,4] and as a function of its

position the intermediate band can appear as a proper band or as a shoulder. For our purposes, we selected the synthetic parameters in order to obtain GNS with the long band centred at 800 (±30) nm. A TEM image of a typical GNS preparation used in this work is reported in Fig S1 in Supplementary Data.

The position of the GNS LSPR bands will shift upon the addition of thiols, due to the change of the local refractive index experienced by GNS when displacing the labile LSB double layer with thiolated molecules,[17,18,28] a phenomenon that is particularly evident for the long band. We thus performed spectrophotometric titrations on aliquots of the standard GNS colloid with the two thiols we planned to use, MMC and HS-PEG_{3000}-NH_2, obtaining that in both cases that a concentration of 1.1 (±0.2) x 10^{-5} M of thiol was needed to give a monolayer on GNS, as we already observed for other thiols.[17] An example of titration profile obtained from one of the experiments (repeated five times) is reported in Figure S2 (see Supplementary Data). At this overall concentration, when using a mixture of two thiols in the coating solution, the composition of the mixture in the coating solution is conserved also on the nano-objects surface: with this simple "trick" it is easy to obtain on the GNS surface a mixed monolayer with a known composition of the two chosen thiols.

From the spectrophotometric titrations we also found that for the long band a red shift of 8 (±2) nm is observed, when coating with a monolayer of HS-PEG_{3000}-NH_2, while the formation of a monolayer of MMC was confirmed[17] to induce a red-shift of 31 (±2) nm. It is worth of note that when coating a colloidal suspension of this kind of nano-objects with a mixture of two different thiols in the described conditions corresponding to the formation of a monolayer on the whole available colloidal surface, the red shift observed should be the result of a linear combination between the two red-shift values observed when coating the colloid surface with each single thiol. The overall behaviour described so far thus allows to check quite precisely the surface composition when using a mixture of different coating agents (and thus of different functions) on noble metal nano-objects in a straightforward way. In order to check this aspects, we measured the spectra of GNS coated with different compositions of mixtures of the two thiols (at an overall concentration of 1.1 x 10^{-5} M), obtaining a good linear regression, with R^2 = 0.9823 (experiment repeated five times, see Figure S3 in Supplementary Data).[17]

At this point, we decided to coat GNS with a mixture of 25% of MMC and 75% of HS-PEG_{3000}-NH_2, in order to emphasize the number of amino groups that could be coupled with FA, but in the same time keeping a surface concentration of MMC able to give a SERS response intense enough to allow for clear SERS imaging. Thus, after purification of GNS from excess of LSB by ultra-centrifugation, the stock solution of the coating mixture was added in the proper amount to

the colloid. As expected from the linear relationship described in Figure S3, a red-shift of about 15 nm was observed after the coating, demonstrating the controllability of the coating process.[17]

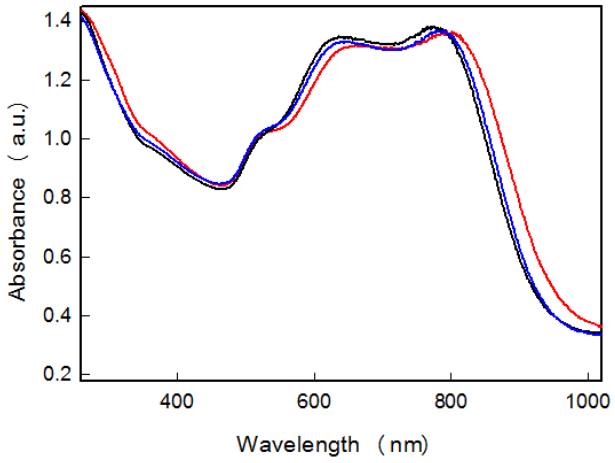

Figure 1: Uv-vis-NIR spectra of: native GNS (black line), GNSs coated with 25% MMC 75% HS-PEG_{3000}-NH_2 (blue line), with 25% MMC 75% HS-PEG_{3000}-NH_2 after coupling with folic acid (FA-GNS, red line).

The obtained colloidal suspension of GNS coated with 25% MMC and 75% HS-PEG_{3000}-NH_2 was reacted overnight in presence of a solution of FA activated with NHS/EDC. After two cycles of ultra-centrifugation and re-dissolution in ultrapure water, the FA functionalized GNS (FA-GNS) were characterized. UV-Vis spectra demonstrated that the reaction did not affect the morphology of the colloid, as the shape of LSPR absorption is completely conserved. A red-shift of 19(±1) nm of the long band is observed (see Figure 1, red line) moving from the coated GNS to FA-GNS, indicating that a sensible change on the GNS surface features, causing a variation of local refractive index, has took place upon the coupling reaction with FA.

Another convincing indication comes from Z-potential measurements as a function of pH. 25% MMC / 75%NH_2 coated GNS show positive values of Z-potential at acidic pH, as in these conditions their surface is positively charged: the terminal amino groups of PEG groups are protonated as -NH_3^+. At pH values higher than 8, the Z-potential decreases to values close to zero, as an effect of deprotonation of -NH_3^+ groups. Moving to FA-GNS, a neat change in the trend is observed. As it can be seen from Figure 2, Z-potential of FA-GNS (grey diamonds) is negative for pH higher than 5, while moving towards acidic pH values it becomes close to zero, in correspondence with the protonation of carboxylates. FA, in fact, possess two carboxylic

functions: one of the two is expected to give the coupling reaction with the amino group of the HS-PEG_{3000}-NH_2 coating agent bound to GNS, while the other remains free on the nano-objects. So, after the coupling reaction, GNS do not expose amino groups anymore, substituted by carboxylic functions of FA. The clear change of Z-potential in the whole pH range is consistent with this interpretation.

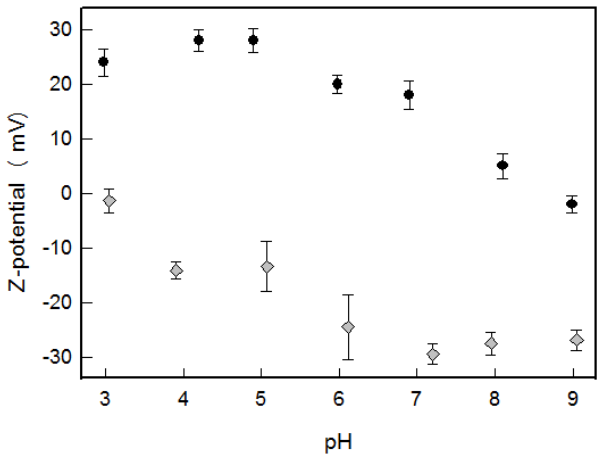

Figure 2: Z-potential titrations of GNSs coated with 25% MMC 75% HS-PEG_{3000}-NH_2 (black dots) or with 25% MMC 75% HS-PEG_{3000}-NH_2 after coupling with folic acid (FA-GNS, grey diamonds).

IR spectra confirm again the success of the coupling reaction. In order to avoid interferences of MMC bands in IR spectra, we synthesised GNS having a coating with 100% of HS-PEG_{3000}-NH_2, and then we reacted them with FA in the same conditions already described. In the spectrum of purified 100% FA-GNS the clear presence of two bands typical of amidic functions (1700 cm^{-1} and 1608 cm^{-1}, respectively C=O stretching and N-H bending) can be observed (see Figure S4 in Supplementary Data), which are absent in the 100% HS-PEG_{3000}-NH_2 coated GNS.

3.2 MTT assay

The MTT Cell Proliferation Assay measures the cell proliferation rate and conversely, when metabolic events lead to apoptosis or necrosis, the reduction in cell viability. In order to evaluate the cytotoxicity of FA-GNS towards HeLa cells, a MTT assay was designed. Before this, an ICP-OES analysis was realized on the FA-GNS colloids used, in order to measure the concentration of gold and of nano-objects. The value found for gold is 1.9×10^{-4} M (0,037 mg/mL), that corresponds to a GNS concentration of 1.2×10^{-9} M (the estimate average mass of

a GNS is 5×10^{-17} g/GNS).[17] Based on this information, the MMT experiment was performed: FA-GNS were suspended into the medium in order to obtain gold concentrations of 5, 10, 25, 50, 100 µg/mL. The values of cells viability are reported in Figure 3. The data show that, for each explored concentration, the cells viability does not change with respect to control cells, thus indicating that FA-GNS can be considered entirely biocompatible in the investigated range. Moreover, we controlled the LSPR spectra before and after the incubation period, to monitor the stability of the colloidal suspensions in the medium used and exclude any irreversible aggregation due to salinity. In all cases, except that for the highest concentration (100 µg/mL) used, no changes in LSPR spectra were observed. The value of 100 µg/mL has been excluded because a precipitation phenomenon was observed into the well during the MTT test, thus the value of 50 µg/mL was chosen.

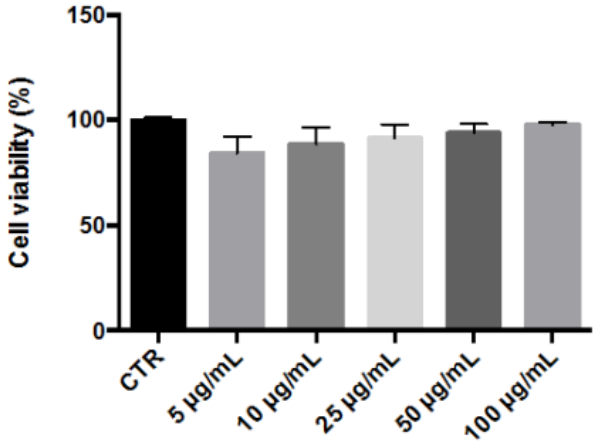

Figure 3: Cell viability of HeLa cells following incubation for 24 hours with FA-GNS at different concentrations. Data are expressed as percentage with respect to control (CTR: 100%).

3.3 Behavior of FA-GNS as SERS tags

The SERS spectra from MMC in a colloidal suspensions of FA-GNS is reported in the region 1100 cm^{-1}-1900 cm^{-1} in Figure S5. The signal is the typical Raman fingerprint of MMC[17,18] with two main bands at 1170 and 1600 cm^{-1}, the latter due to the C=C stretching inside lactone and benzene rings.[29] The mode at close to 1600 cm^{-1} has been used to derive the EF: the integrated intensity has been calculated by best fitting procedure and then compared with the same parameter from a solution of MMC in ethanol, as already described in our precedent

work.[17] Being the experiments performed in the same conditions and geometry and considering the concentration ratio and the values for integrated intensities, we obtained an EF about 10^5-10^6. The SERS spectra measured on a sample of a purified FA-GNS colloid demonstrates that the reaction steps used for the functionalization with FA of the nano-devices did not affect their SERS performances (see Figure S5 in Supplementary Data).

FA-GNS described so far should be able to recognize and bind cells that overexpress folate receptors. HeLa cells are an immortal cell line, derived from cervical cancer cells, that present this feature, so they were used to evaluate the ability of FA-GNS to recognize and localize folate receptors, thanks to the relative SERS signal. Recently, we demonstrated the ability of nano-devices, based on identical GNS protected with PEG-thiols and overcoated with a positive external layer of polyallylamine hydrochloride (PAH), to be internalized by SH-SY5Y cells and revealed by Two Photon Luminescence[30] and SERS imaging.[17]

FA-GNS were used for incubation of HeLa cells (30000 cells/mL) for 24 hours at 37°C. Then, after careful washing in order to remove all FA-GNS not bound to membranes, the SERS response was evaluated along a line of 21 μm moving from outside entering in the cell across the membrane, located approximately between 12 and 15 microns from the starting point, with a step of 1.5 microns. The measure is summarized in the graph reported in Figure 4a (blue circles), which plots the integrated intensity measured for the Raman mode at 1600 cm^{-1} versus the spot position.

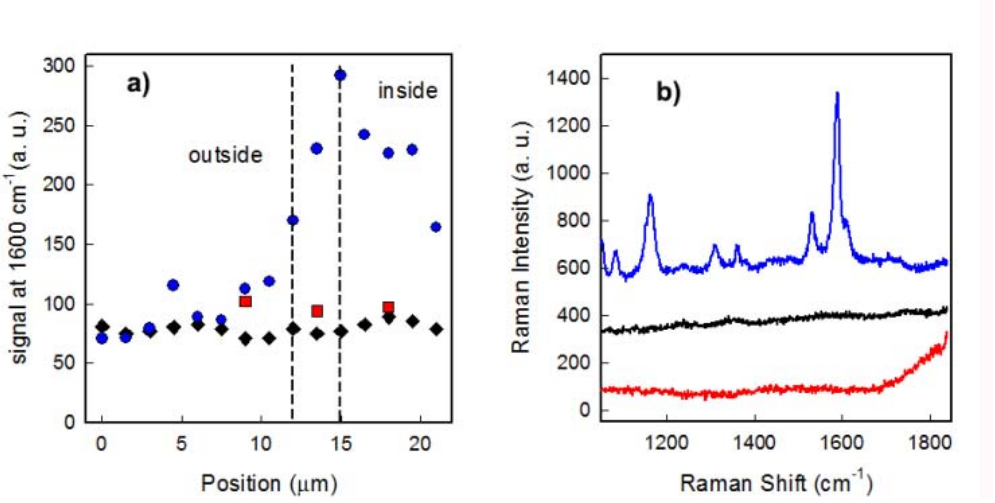

Figure 4: a) Comparison between SERS response of: (blue circles) HeLa cells incubated with FA-GNS; (black diamonds) Hela cells incubated with GNS coated with 75% HS-PEG-COOH and 25% MMC; (red squares) DI TCN1 cells incubated with FA-GNS evaluated in three distinct points outside the cell, on the membrane and inside the cell. The region between the two vertical dashed lines represent a sampling zone corresponding to the membranes for all the

investigated cells. b) The average of four spectra taken on four different points on the membrane cells after incubation with SERS tags: (blue line) HeLa cells incubated with FA-GNS; (black line) Hela cells incubated with GNS coated with 75% HS-PEG-COOH and 25% MMC; (red line) DI TCN1 cells incubated with FA-GNS.

As it can be seen, the MMC signal at 1600 cm^{-1} starts to increase over the background values in the zone between 12 and 15 μm, in correspondence to the membrane of the cell, while it is slightly smaller inside the cell (position > 15 μm). Outside the cell the signal is absent, as expected, and one can only observe almost flat spectra over the whole investigated zone outside the cell. The variation of the MMC signal evidenced by the plot (blue circles) in Figure 4a is a proof that FA-GNS are able to recognize and bind folate receptors overexpressed on the membranes of HeLa cells, otherwise they should have been washed away during the three washing cycles after incubation. The fact that the signal is found at a maximum value on the membrane zone depends on the sampling depth of the microscope and the spherical geometry of the sampled zone, but indeed demonstrates that FA-GNS are bound on the membrane of the investigated cells.

A similar experiment was repeated in the same conditions, but in absence of the FA targeting group. For this task we used GNS coated with a mixed monolayer of 75% HS-PEG-COOH and 25% MMC. We choose this coating as the presence of carboxylic groups give the nano-device a distinctively negative Z-potential[17] (as in the case of FA-GNS), but without the ability to be recognized by folate receptors. HeLa cells were incubated with the coated GNS for 24 hours at 37°C, then washed three times with PBS, and after this the SERS response was evaluated again across the membrane of a HeLa cell. Comparing the result (see black diamonds in Figure 4a) with the plot obtained for FA-GNS it is evident that no presence of SERS tag is observed after incubation and washing: absence of folate on GNS rules out any binding to membranes.

A proof of selectivity of FA-GNS was obtained repeating the incubation for 24 hours at 37°C using DI TCN1 cells, astrocytes with fibroblast shape that do not overexpress folate receptors. In this case, the SERS response was evaluated analyzing 3 points (outside, inside the cell and on the membrane), and the result is reported by the three red squares reported in Figure 4a. As expected, no SERS signal from MMC can be found in any of the regions investigated: FA-GNS were washed away during the three washing cycles, as this kind of cells lack folate receptor and no sensible binding of FA-GNS is possible.

The results of these experiments can be summarized by showing SERS spectra obtained taking four spectra on four different positions on the membranes zone in the cells described in the

three experiments. As it can be seen in Figure 4b, the typical Raman fingerprint of MMC can be observed only on the membrane of the HeLa cancer cells treated with FA-GNS, while this signal is absent in the spectra measured during the other two experiments: no presence of SERS tags on cells membrane is observed as no binding between folate and corresponding receptors can take place. In one case (COOH finished SERS tags) we lack the folate moiety, in the other (DI TCN1 cells) we lack the folate receptors. FA-GNS thus act as specific tags for cancer cells overexpressing folate receptors.

On these bases, we performed a bi-dimensional mapping, taking a grid of spectra along a rectangular area that include a portion of space taken inside and a portion taken outside of a HeLa cell after incubation with FA-GNS and three cycles of washing.

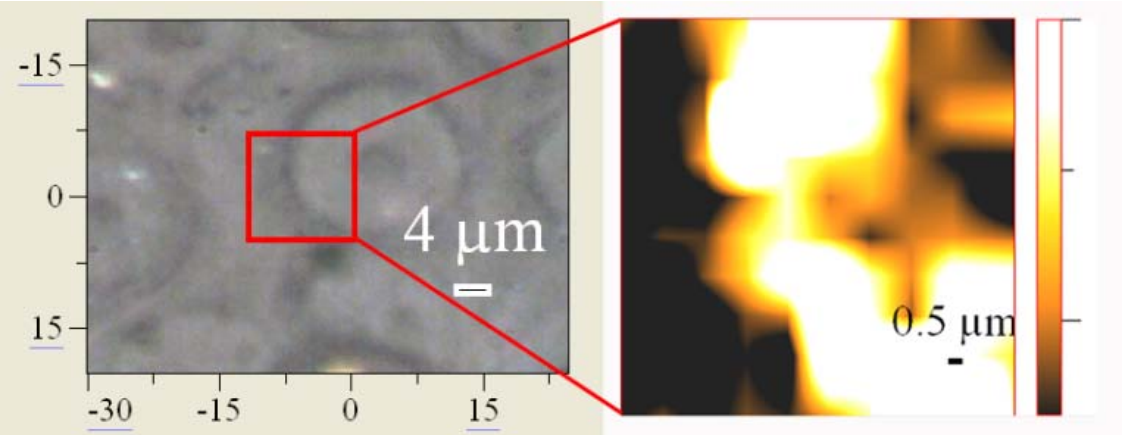

Figure 5: On the left: image of HeLa cells incubated with FA-GNS, characterized at micro-Raman spectroscopy: the red rectangular delimits the area which was mapped with the micro-Raman; on the right: image of the distribution of the integrated intensity of the MMC Raman signal at 1600 cm^{-1}, recorded in the red rectangular area.

As it can be seen from Figure 5, SERS mapping (the brighter the image, the higher is the intensity of the Raman signal at 1600 cm^{-1}) from the area included in the red rectangle allows to recognize the cell, with a very high intensity on the cell border corresponding to the membrane.

3.4 Photothermal treatment of HeLa cells with FA-GNS

After having demonstrated the efficiency of the SERS tags in the recognition and imaging of HeLa cancer cells by means of specific interactions of FA-GNS with membranes overexpressing folate receptors, we were interested in demonstrating the ability to damage the same membranes by means of hyperthermia produced by the photothermal effect exerted by FA-GNS

in close contact. The typical experiment was performed incubating HeLa cells with the SERS tag for 24 hours at 37 °C. After this, samples were washed three times in order to eliminate all FA-GNS which were not bound to cell membranes, and then irradiated with a laser source for 10 minutes at 808 nm, at an irradiance value (0.190 W/cm^2) lower than the safety limit for skin (see experimental).[26]

After irradiation, cells were observed at a conventional optical microscope, and photographs were taken.

As a control, the following samples were considered: i) HeLa cells incubated for 24 hours without SERS tags and without laser irradiation, ii) HeLa cells incubated for 24 hours without SERS tags irradiated for 10 minute; iii) HeLa cells incubated for 24 hours with SERS tags, without laser irradiation.

As it can be clearly seen from Figure 6, in the sample incubated with 50 µg/mL SERS tags and irradiated for 10 minutes the majority of cells (over 80%) underwent a visible transformation, moving from a normal polygonal shape to a roundish shape (Figures 6d and 6f). This is a clear indication of necrotic death process driven by a sudden and irrecoverable cell damage,[31-32] produced by the local hyperthermia generated by irradiated FA-GNS.

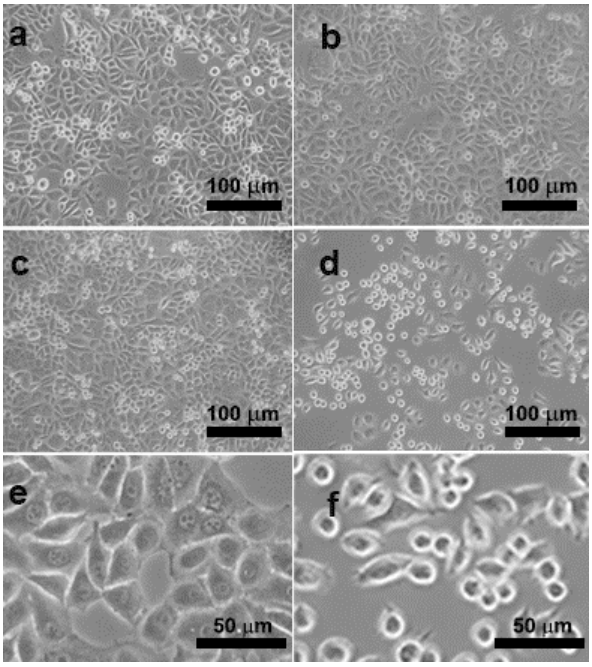

Figure 6: a) HeLa cells culture before incubation and irradiation; b) Hela cells before incubation and after irradiation; c) HeLa cells culture after 24 hours incubation with SERS tags and three cycles of washing, before irradiation; d) HeLa cells culture after 24 hours incubation with SERS

tags and three cycles of washing, after irradiation; e) same as i c), higher magnification; f) same as d), higher magnification

Laser irradiation alone in absence of GNS (Figure 6b), as well as the simple incubation with SERS tags in absence of irradiation (Figure 6c) do not produce any harm to of HeLa cells population, whose aspect is identical to the untreated cells (Figure 6a), with almost complete presence (about 90%) of healthy cells, as expected from MTT studies: in absence of Laser irradiation the GNS concentration of 50 μg/mL is safe for cells. No sensible differences in photo-thermal cell damaging efficiency were observed when reducing the incubation concentration of GNS to 25 μg/mL. Lower concentrations of SERS tags were not investigated: as already reported, SERS intensities of GNS tags bound to cell membranes depends on the concentration used in the incubation, and lowering too much this value could result in poor SERS signals.[17]

4. Conclusions

The presented strategy to build a prototype of theranostic device consisted of several successful steps: (i) choice of the LSPR features of GNS, obtaining a strong absorbance in the NIR, into the biological window; (ii) rational and controlled coating of GNS surface with a tuneable mixture of protecting units and Raman reporters, in order to ensure biocompatibility, stability and an intense SERS signal; (iii) covalent binding of FA to protecting units bound to GNS, imparting selectivity and obtaining a SERS tag able to signal only cells overexpressing folate receptors on their membranes, with reliable imaging features. The new folate-targeted systems are highly biocompatible and allow reaching a high GNS concentration at the site of tumour cells with low systemic exposure. Once on the target, they just need an ultralow irradiation to activate the hyperthermia required to kill cancer cells in vitro. Given the flexibility of this modular approach, we believe that this prototype could be useful for the realization of further and more sophisticated theranostic devices.

Acknowledgment

University of Pavia (Fondo Ricerca Giovani 2015) is kindly acknowledged.

References

1. Boisselier E and Astruc D 2009 Gold nanoparticles in nanomedicine: preparations, imaging, diagnostics, therapies and toxicity. *Chem.Soc. Rev.* **38** 1759-1782.
2. Li N, Zhao PX and Astruc D 2014 Anisotropic Gold Nanoparticles: Synthesis, Properties, Applications, and Toxicity. *Angewandte Chemie-International Edition* **53**, 1756-1789
3. Pallavicini P, Dona A, Casu A, Chirico G, Collini M, Dacarro G, Falqui A, Milanese C, Sironi L and Taglietti A 2013 Triton X-100 for three-plasmon gold nanostars with two photothermally active NIR (near IR) and SWIR (short-wavelength IR) channels. *Chem. Comm.* 2, **49**, 6265
4. Casu A, Cabrini E, Dona A, Falqui A, Diaz-Fernandez Y, Milanese C, Taglietti A and Pallavicini P 2012 Controlled Synthesis of Gold Nanostars by Using a Zwitterionic Surfactant *Chem. Eur. J*. **18**, 9381
5. Wang YQ, Yan B and Chen LX 2013 SERS Tags: Novel Optical Nanoprobes for Bioanalysis *Chem. Rev.* **113**, 1391-1428
6. Van de Broek B, Devoogdt N, D'Hollander A, Gijs HL, Jans K, Lagae L, Muyldermans S, Maes G and Borghs G 2011 Specific Cell Targeting with Nanobody Conjugated Branched Gold Nanoparticles for Photothermal Therapy *ACS Nano*, **5**, 4319-4328
7. Dreaden EC, Alkilany AM, Huang XH, Murphy CJ and El-Sayed MA 2012 The golden age: gold nanoparticles for biomedicine. *Chem. Soc. Rev.*, **41**, 2740-2779
8. Ma Y, Liang XL, Tong S, Bao G, Ren QS and Dai ZF 2013 Gold Nanoshell Nanomicelles for Potential Magnetic Resonance Imaging, Light-Triggered Drug Release, and Photothermal Therapy *Adv. Funct. Mater.*, **23**, 815-822
9. Tian QW, Hu JQ, Zhu YH, Zou RJ, Chen ZG, Yang SP, Li RW, Su QQ, Han Y and Liu XG 2013 Sub-10 nm Fe3O4@Cu2-xS Core-Shell Nanoparticles for Dual-Modal Imaging and Photothermal Therapy *J. Am. Chem. Soc.*, **135**, 8571-8577
10. Ma Y, Tong S, Bao G, Gao C and Dai ZF 2013 Indocyanine green loaded SPIO nanoparticles with phospholipid-PEG coating for dual-modal imaging and photothermal therapy *Biomaterials*, **34** 7706-7714
11. Yang K, Zhang SA, Zhang GX, Sun XM, Lee ST and Liu ZA 2010 Graphene in Mice: Ultrahigh In Vivo Tumor Uptake and Efficient Photothermal Therapy *Nano Lett.* **10**, 3318-3323
12. Gao YP, Li YS, Chen JZ, Zhu SJ, Liu XH, Zhou LP, Shi P, Niu DC, Gu JL and Shi JL 2015 Multifunctional gold nanostar-based nanocomposite: Synthesis and application for noninvasive MR-SERS imaging-guided photothermal ablation *Biomaterials*, **60**, 31-41
13. Seo SH, Kim BM, Joe A, Han HW, Chen XY, Cheng Z and Jang ES 2014 NIR-light-induced surface-enhanced Raman scattering for detection and photothermal/photodynamic therapy of

cancer cells using methylene blue-embedded gold nanorod@SiO2 nanocomposites *Biomaterials*, **35**, 3309-3318

14. Wang XC, Li GH, Ding Y and Sun SQ 2014 Understanding the photothermal effect of gold nanostars and nanorods for biomedical applications *Rsc Adv.* **4**, 30375-30383
15. Huang P, Pandoli O, Wang XS, Wang Z, Li ZM, Zhang CL, Chen F, Lin J, Cui DX and Chen XY 2012 Chiral guanosine 5'-monophosphate-capped gold nanoflowers: Controllable synthesis, characterization, surface-enhanced Raman scattering activity, cellular imaging and photothermal therapy, *Nano Res.*, **5**, 630-639
16. Lu WT, Singh AK, Khan SA, Senapati D, Yu HT and Ray PC 2010 Gold Nano-Popcorn-Based Targeted Diagnosis, Nanotherapy Treatment, and In Situ Monitoring of Photothermal Therapy Response of Prostate Cancer Cells Using Surface-Enhanced Raman Spectroscopy *J. Am. Chem. Soc.*, **132**, 18103-18114
17. Bassi B, Taglietti A, Galinetto P, Marchesi N, Pascale A, Cabrini E, Pallavicini P and Dacarro G 2016 Tunable coating of gold nanostars: tailoring robust SERS labels for cell imaging *Nanotechnology* **27**, 265302
18. Taglietti A, Fernandez YAD, Galinetto P, Grisoli P, Milanese C and Pallavicini P 2013 Mixing thiols on the surface of silver nanoparticles: preserving antibacterial properties while introducing SERS activity *J. Nanopart. Res.* **15**, 1–13
19. Stewart A, Zheng S, McCourt MR and Bell SEJ 2012 Controlling Assembly of Mixed Thiol Mono layers on Silver Nanoparticles to Tune Their Surface Properties *ACS Nano* **6**, 3718-3726
20. Fasolato C, Giantulli S et al. 2016 Folate-based single cell screening using surface enhanced Raman microimaging *Nanoscale*, 2, **8**, 17304-17313
21. Kim SL, Jeong HJ, Kim EM, Lee CM, Kwon TH and Sohn M 2007 Folate receptor targeted imaging using poly (ethylene glycol)-folate: In in vitro and in vivo studies *J. Korean Med. Sci.* **22**, 405-411
22. Wang S and Low PS 1998 Folate-mediated targeting of antineoplastic drags, imaging agents, and nucleic acids to cancer cells. Journal of Controlled Release, *Journal of Controlled Release* **53**, 39-48
23. Bhattacharya R, Patra CR et al. 2007 Attaching folic acid on gold nanoparticles using noncovalent interaction via different polyethylene glycol backbones and targeting of cancer cells *Nanomedicine* **3**, 224-238
24. P.C. Elwood 1989 MOLECULAR-CLONING AND CHARACTERIZATION OF THE HUMAN FOLATE-BINDING PROTEIN CDNA FROM PLACENTA AND MALIGNANT-TISSUE CULTURE (KB) CELLS *J. Biol. Chem.* **264**, 14893-14901

25. Boca-Farcau S, Potara M, Simon T, Juhem A, Baldeck P and Astilean S 2014 Folic Acid-Conjugated, SERS-Labeled Silver Nanotriangles for Multimodal Detection and Targeted Photothermal Treatment on Human Ovarian Cancer Cells *Mol. Pharm.* **11**, 391-399
26. Yuan H, Fales AM and Vo-Dinh T 2012 TAT Peptide-Functionalized Gold Nanostars: Enhanced Intracellular Delivery and Efficient NIR Photothermal Therapy Using Ultralow Irradiance *J. Am. Chem. Soc.***134**, 11358-11361
27. Osera C, Martindale JL et al 2015 Induction of VEGFA mRNA translation by CoCl2 mediated by HuR *RNA Biol.* **12**, 1121-1130
28. Amato E, Diaz-Fernandez YA, Taglietti A, Pallavicini P, Pasotti L, Cucca L, Milanese C, Grisoli P, Dacarro C, Fernandez-Hechavarria JM and Necchi V 2011 Synthesis, Characterization and Antibacterial Activity against Gram Positive and Gram Negative Bacteria of Biomimetically Coated Silver Nanoparticles *Langmuir* **27**, 9165-9173
29. Vogel E and Kiefer W 1998 Investigation of the metal adsorbate interface of the system silver coumarin and silver hydrocoumarin by means of surface enhanced Raman spectroscopy. *Fresenius J Anal. Chem.* **361**, 628-630
30. Pallavicini P, Cabrini E, Cavallaro G, Chirico G, Collini M, D'Alfonso L, Dacarro G, Donà A, Marchesi N and Milanese C 2015 Gold nanostars coated with neutral and charged polyethylene glycols: A comparative study of in-vitro biocompatibility and of their interaction with SH-SY5Y neuroblastoma cells *J. of Inorg. Biochem.***151**, 123-131
31. Villanueva A, Vidania R, Stockert JC, Cañete M and Juarranz A, 2003 Handbook of Photochemistry and Photobiology, Vol. 4, ed. H. S. Nalwa, American Scientific Publishers, California, pp. 79–117
32. Rello S, Stockert JC, Moreno V, Gamez A, Pacheco M, Juarranz A, Canete M and Villanueva A 2005 Morphological criteria to distinguish cell death induced by apoptotic and necrotic treatments *Apoptosis*, **10**, 201-208